

Disorder-immune coupled resonator optical waveguide

Alexey G. Yamilov and Massimo F. Bertino

Department of Physics, University of Missouri–Rolla, Rolla, Missouri 65409, USA

Received August 14, 2006; revised November 6, 2006; accepted November 8, 2006;
posted November 8, 2006 (Doc. ID 74019); published January 12, 2007

We demonstrate that a photonic lattice with short- and long-range harmonic modulations of the refractive index facilitates formation of flat photonic bands and leads to slow propagation of light. The system can be considered a coupled-resonator optical waveguide (CROW): photonic bands with abnormally small dispersion are created due to the interaction of long-lived states in the cavity regions via weak coupling across tunneling barriers. Unlike previous CROW implementations, the proposed structures can be fabricated with interference photolithography (holography), sidestepping the issue of resonator-to-resonator fluctuation of the system parameters. The proposed holography-based approach enables fabrication of arrays with a large number of coupled optical resonators, which is necessary for practical applications. © 2007 Optical Society of America

OCIS codes: 230.4000, 230.5750, 250.5300.

Photonic crystal (PhC) structures¹ have been recognized as a versatile testbed for achieving unparalleled control over light propagation, including slowing down or stopping light completely, that can be used in, e.g., optical memories, delay lines, and to enhance nonlinear interactions. Among the solid-state approaches to slowing down light,² periodic arrays of weakly coupled resonators show great promise.³ Such an array,⁴ dubbed a coupled-resonator optical waveguide^{5,6} (CROW), is essentially a one-dimensional (1D) PhC with a carefully engineered photonic band structure. Hybridization of the high- Q resonances of the individual cavities leads^{5,6} to a low-dispersion photonic band:

$$\omega(K) = \Omega[1 + \kappa \cos(Ka)]. \quad (1)$$

The propagation speed of a light pulse at frequencies within the band can be considerably reduced ($v_g = d\omega/dK \ll c$) when the coupling between the resonators is weak (small κ). Efficient second-harmonic generation⁷ and high-power low-threshold lasers⁸ are among the possible applications of CROW devices. To make a CROW practical, it needs to contain a large number of the individual resonators. However, hybridization of high- Q resonances of the individual resonators is possible only when the latter are nearly identical. This requirement puts severe constraints on the fabrication error margin and the resonator-to-resonator parameter fluctuation tolerance. Difficulty in satisfying these strict criteria has hampered widespread applications of CROW devices.³

Here we demonstrate that this limitation can be sidestepped in 1D PhC that possesses a long-range (α_L) harmonic modulation of the refractive index (see Fig. 1):

$$n^2(x) = \epsilon(x) = \epsilon_0 + \Delta\epsilon[\alpha \cos(k_1x) + \beta \cos(k_2x)]^2, \quad (2)$$

where $k_1 - k_2 \equiv \Delta k$, $(k_1 + k_2)/2 \equiv k$, and $\alpha + \beta = 1$. k and Δk are related to the short- and long-range modulations of the refractive index: $\alpha_S = 2\pi/\Delta k$ and $\alpha_L = \pi/k$, respectively.

Flat bands related to the periodically placed structural defects (resonators) in 1D PhCs have been observed^{9–12} and considered for CROW applications.^{13,14} However, the structures proposed before need to be constructed with the layer-by-layer technique, which is susceptible to fabrication errors, as are the other CROWs discussed above. We propose to use optical holography to create dual-harmonic modulations of the refractive index as in Eq. (2). Holography is a mature technique that can be used in conjunction with, e.g., quantum dot lithography¹⁵ to define a dual-periodic PhC CROW with a large number of virtually identical resonators. Furthermore, we demonstrate that our approach allows easy control of the optical properties of the CROW.

Let us consider four s -polarized laser beams defined by

$$\begin{bmatrix} \mathbf{q}_{L1}, E_{L1} \\ \mathbf{q}_{L2}, E_{L2} \\ \mathbf{q}_{R1}, E_{R1} \\ \mathbf{q}_{R2}, E_{R2} \end{bmatrix} = \begin{bmatrix} k_0\{-\sin(\theta_1), 0, \cos(\theta_1)\}, E_1 \\ k_0\{-\sin(\theta_2), 0, \cos(\theta_2)\}, E_2 \\ k_0\{\sin(\theta_1), 0, \cos(\theta_1)\}, E_1 \\ k_0\{\sin(\theta_2), 0, \cos(\theta_2)\}, E_2 \end{bmatrix}. \quad (3)$$

Here \mathbf{q} and E are the k -vector and amplitude of the beams, respectively. Their interference pattern, $E_{\text{tot}}(x) \propto \alpha \cos(k_1x) + \beta \cos(k_2x)$, leads to Eq. (2). The parameters in Eqs. (2) and (3) are related as $\alpha = E_1/(E_1 + E_2)$, $\beta = E_2/(E_1 + E_2)$ and $k_1 = k_0 \sin \theta_1$, $k_2 = k_0 \sin \theta_2$. Manipulation of the beams allows for easy control over the structural properties of the resultant PhC: (i) fundamental periodicity α_S via k_0 and $\theta_{1,2}$; (ii) long-range modulation α_L via $\theta_1 - \theta_2$; (iii) depth of the long-range modulation via the relative intensity of the beams, E_1/E_2 .

Now we show that the proposed long-range refractive index modulation creates alternating spatial regions that can serve as resonators separated by tunneling barriers. The condition of weak coupling $\kappa \ll 1$ between the states of the neighboring resonators requires sufficiently large barriers and therefore $\alpha_S \ll \alpha_L$, which we assume hereafter.

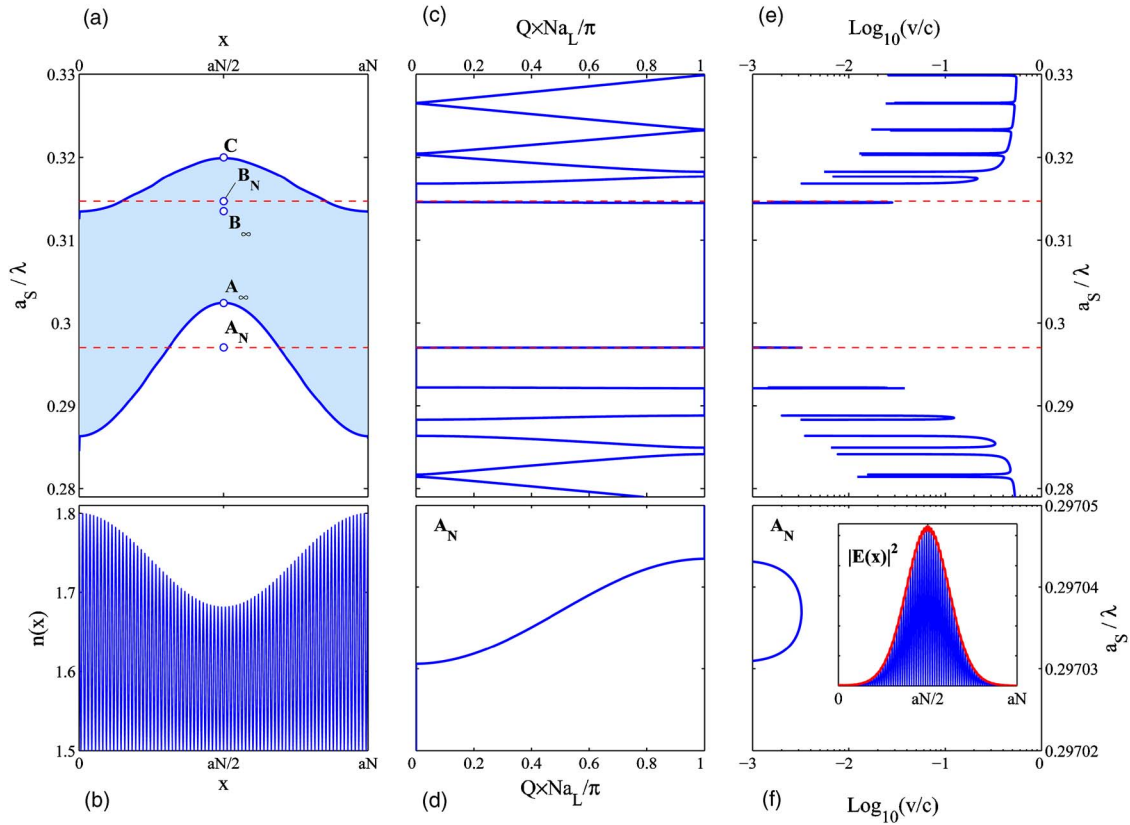


Fig. 1. (a) Photonic bandgap diagram (local PBG) of the dual-periodic photonic crystal lattice defined by Eq. (1) and shown in (b). We used $\epsilon_0=2.25$, $\Delta\epsilon=0.99$, $N=80$, and asymmetry parameter $E_1/E_2=7.5$. A_N and B_N mark the frequencies of the foremost photonic bands on the long- and short-wavelength sides, respectively, of the compound PBG, which extends from A_∞ to B_∞ when $N \rightarrow \infty$. (c) Calculated photonic band structure ($N=80$). The A_N band shows typical cosine dependence as in Eq. (1) dispersion (d). Plot (e) of the group velocity for the series of bands approaching the compound PBG shows the monotonic decrease (notice the logarithmic scale) toward the gap. As discussed in the text, we attribute this trend to (i) the decrease of the local group velocity inside the resonator regions and (ii) the decrease in tunneling coupling between the resonators. (f) Group velocity in the A_N band shown in (d); the inset shows the distribution of intensity (over one period) for the band-edge frequency within the band A_N .

In a regular ($a_L \rightarrow \infty$) 1D PhC, the eigenfunctions of the crystal satisfy the Bloch theorem:

$$E(\omega, x) = e(\omega, x) \times \exp[iK(\omega)x], \quad (4)$$

where $e(\omega, x)$ is periodic on the a_S scale and the eigenfrequency ω enters as a parameter. The propagation of electromagnetic waves over one period in the 1D PhC can be described by a 2×2 transfer matrix^{16–18} $\hat{T}_{\text{tot}} = \Pi_x^{x+a_S} \hat{T}(\zeta, \zeta + d\zeta)$, which is related to the propagation constant $K(\omega)$ as $\cos[K(\omega)a_S] = \text{Tr}[\hat{T}_{\text{tot}}]/2$. In the spectral regions of a photonic bandgap (PBG), $K(\omega)$ becomes complex and wave propagation is possible only via a tunneling mechanism in a PhC of finite length.

In PhCs with long-range modulation, the Bloch theorem Eq. (4) cannot be applied locally on the a_S scale, because now the propagation constant becomes a function of position $K_{\text{loc}}(\omega, x)$. The forward-propagating (locally) wave $\exp[iK_{\text{loc}}(\omega, x)x]$ scatters into $\exp[-iK_{\text{loc}}(\omega, x)x]$, which can be described with the coupled mode approach.^{17,19}

The shaded area in Fig. 1(a) shows the spectral region where K_{loc} becomes complex. This modulation of the PBG as a function of the spatial coordinate [com-

pare with Fig. 1(b) for guidance] allows the electromagnetic wave to propagate with real or imaginary K_{loc} in different parts of the same PhC. As shown in Fig. 1, there exist photonic bands such as A_N or B_N that correspond to the CROW picture: within these bands an EM wave propagates via a tunneling mechanism between the resonator regions. In the case of A_N (B_N) regions around $x_m = Na_S/2 + Na_S \times m$ ($x_m = Na_S \times m$) represent the periodically placed resonators separated by the confining buffers. Here, m is an integer.

For rigorous calculation of the photonic band structure of the dual-periodic system, the transfer matrix over a period is required. An interesting situation may arise when a_L/a_S is noninteger. The spectrum of such a structure exhibits a “butterfly” structure,¹¹ similar to the spectrum of an electron in a solid with an applied magnetic field.²⁰ We, however, will limit our consideration to a special class of commensurate lattices where $a_L/a_S = N$. In this case a_L is a period of the crystal and the spectrum determined by $\cos[K(\omega)a_L] = \text{Tr}[\Pi_x^{x+a_L} \hat{T}(\zeta, \zeta + d\zeta)]/2$.

Figures 1(c)–1(f) show the calculated band structure in the dual-periodic 1D PhC with $N=80$. A series of progressively flatter bands develops on each side of

the PBG region. We offer a clear physical explanation of this effect. For concreteness we will describe the lower-frequency sequence of bands. At frequencies below A_∞ propagation of EM waves is allowed in the vicinity of $x_m = Na_S/2 + Na_S \times m$, leading to the formation of a series of photonic band-edge modes. These modes [see the inset of Fig. 1(f) for the field distribution within the A_N band] hybridize and form photonic bands as in the other CROW implementations.³ $K(\omega)$ can also be related to the transmission coefficient through the single period of the structure¹⁸ $\cos[K(\omega)a_L] = \text{Re}[t(\omega)]$. For a state with a sufficiently high Q , $t(\omega)$ is described by a Lorentzian, $(-1)^N(\Gamma/2)/[i(\Gamma/2) - (\omega - \Omega)]$. Substitution of this expression into the above equation leads directly to Eq. (1) with

$$\kappa = \Gamma/2\Omega \equiv 1/Q. \quad (5)$$

Thus, the decrease of group velocity in the PhC is directly related to the increase of the cavities' Q -factor. Similar to what occurs with the other CROWs, this effect also leads to the reduction of the useful bandwidth, as reviewed in Ref. 3.

In a finite single-periodic PhC, the Q -factor of the band-edge mode depends on the system size. In our case a_L gives the characteristic length, which also determines the frequency of the last (closest to the band-edge) mode, A_N . As N increases, A_N shifts toward A_∞ because the size of each resonator region increases [see also the inset of Fig. 1(f)]. The decrease of the local group velocity $v_g(x) = [dK_{\text{loc}}(\omega, x)/d\omega]^{-1}$ around $x_m = Na_S/2 + Na_S \times m$ contributes to the increase of the Q -factor of the resonators.

The other factor that affects confinement is the tunneling rate between consecutive cavities. This can be controlled in the considered dual-periodic PhC by $\Delta\epsilon$ and/or by the depth of the long-range modulation set by α (or β), Eq. (2). If the former may not be adjustable for the given experimental conditions, the latter is easily controlled by changing the relative intensity of the pairs of lithographic beams, E_1/E_2 . One may expect that 100% modulation [$\alpha = \beta = 1/2$ in Eq. (2)] should lead to the photonic bands with the smallest dispersion (smallest group velocity). In this case, however, the resonators located at $x_m = Na_S/2 + Na_S \times m$ would consist of the spatial regions with an almost constant refractive index and thus $v_g(x) \sim c$. Furthermore, complete modulation would also negatively affect (increase) the coupling between the resonators. This can also be seen from PBG diagram in Fig. 1(a): points A_∞ and C would coincide as a result of the $\alpha = \beta = 1/2$ condition. Therefore, the frequency of the A_N state would fall into the region where there is no PBG at $x_m = Na_S \times m$ positions. Indeed, our photonic band structure calculations demonstrate that structures with 100% modulation are less advantageous and lead to significantly larger propagation speeds. The optimum value of α depends on the experimental parameters (ϵ_0 , $\Delta\epsilon$, and N) and should be determined with the help of a PBG diagram similar

to Fig. 1(a). The diagram also proves useful in explaining the advantage of A_N over B_N . In the latter case, the tunneling barriers are thinner and their localization length is longer (PBG is spectrally narrower at $x_m = Na_S/2 + Na_S \times m$ than it is at $x_m = Na_S \times m$).

In summary, there are numerous applications that can take advantage of slow-propagating light: optical memories, low-threshold lasers, nonlinear devices, and delay lines. Experimental realizations of CROW slow-light devices, suffer from low structural-error tolerances. Unlike previously known resonators, the proposed photonic crystal lattice with dual-harmonic modulations of the refractive index defined by Eq. (2) can be implemented by interference lithography of four plane-wave beams, ensuring that all resonators and tunneling barriers are the same. This approach paves the way to inexpensive slow-light applications.

A. Yamilov (yamilov@umr.edu) acknowledges support from University of Missouri–Rolla.

References

1. C. M. Soukoulis, *Photonic Band Gap Materials* (Kluwer, 1996).
2. P. W. Milonni, *Fast Light, Slow Light and Left Handed Light* (Institute of Physics, 2005).
3. See J. Scheuer, G. Paloczi, J. Poon, and A. Yariv, *Opt. Photon. News* **16**(2), 36 (2005) and references therein.
4. N. Stefanou and A. Modinos, *Phys. Rev. B* **57**, 12127 (1998).
5. A. Yariv, Y. Xu, R. K. Lee, and A. Scherer, *Opt. Lett.* **24**, 711 (1999).
6. J. K. S. Poon, L. Zhu, G. A. DeRose, and A. Yariv, *J. Lightwave Technol.* **24**, 1843 (2006).
7. Y. Xu, R. K. Lee, and A. Yariv, *J. Opt. Soc. Am. B* **17**, 3870 (2000).
8. H. Altug and J. Vuckovic, *Appl. Phys. Lett.* **86**, 111102 (2005).
9. R. Shimada, T. Koda, T. Ueta, and K. Ohtaka, *J. Appl. Phys.* **90**, 3905 (2001).
10. H. Kitahara, T. Kawaguchi, J. Miyashita, R. Shimada, and M. W. Takeda, *J. Phys. Soc. Jpn.* **73**, 296 (2004).
11. R. Shimada, T. Koda, T. Ueta, and K. Ohtaka, *J. Phys. Soc. Jpn.* **67**, 3414 (1998).
12. Z.-W. Liu, Y. Du, J. Liao, S.-N. Zhu, Y.-Y. Zhu, Y.-Q. Qin, H.-T. Wang, J.-L. He, C. Zhang, and N.-B. Ming, *J. Opt. Soc. Am. B* **19**, 1676 (2002).
13. M. Bayindir, S. Tanriseven, and E. Ozbay, *Appl. Phys. A* **72**, 117 (2001).
14. M. Bayindir, C. Kural, and E. Ozbay, *J. Opt. A* **3**, 184 (2001).
15. M. F. Bertino, R. R. Gadipalli, J. G. Story, C. G. Williams, G. Zhang, C. Sotiriou-Leventis, A. T. Tokuhito, S. Guha, and N. Leventis, *Appl. Phys. Lett.* **85**, 6007 (2004).
16. P. Yeh, *Optical Waves in Layered Media* (Wiley, 2005).
17. J. E. Sipe, L. Poladian, and C. Martin de Sterke, *J. Opt. Soc. Am. A* **11**, 1307 (1994).
18. J. M. Benedickson, J. P. Dowling, and M. Scalora, *Phys. Rev. E* **53**, 4107 (1996).
19. D. Janner, G. Galzerano, G. Della Valle, P. Laporta, S. Longhi, and M. Belmonte, *Phys. Rev. E* **72**, 056605 (2005).
20. D. R. Hofstadter, *Phys. Rev. B* **14**, 2239 (1976).